



## Physicochemical and environmental properties of arsenic sulfide sludge from copper and lead–zinc smelter

Li-wei YAO<sup>1</sup>, Xiao-bo MIN<sup>1,2</sup>, Hui XU<sup>1</sup>, Yong KE<sup>1,2</sup>, Yun-yan WANG<sup>1,2</sup>,  
Zhang LIN<sup>1,2</sup>, Yan-jie LIANG<sup>1,2</sup>, De-gang LIU<sup>1</sup>, Qiu-jing XU<sup>1</sup>, Yu-yang HE<sup>1</sup>

1. School of Metallurgy and Environment, Central South University, Changsha 410083, China;

2. Chinese National Engineering Research Center for Control & Treatment of Heavy Metal Pollution,  
Central South University, Changsha 410083, China

Received 10 October 2019; accepted 18 May 2020

**Abstract:** Physicochemical properties of arsenic sulfide sludge (ASS) from copper smelter (ASS-I) and lead–zinc smelter (ASS-II) were examined by XRD, Raman spectroscopy, SEM–EDS, TG–DTA, XPS and chemical phase analysis method. The toxicity characteristic leaching procedure (TCLP), Chinese standard leaching tests (CSLT), three-stage sequential extraction procedure (BCR) and batch leaching experiments (BLE) were used to investigate the environmental stability. The ASSs from different smelters had obviously different physicochemical and environmental properties. The phase composition and micrograph analysis indicate that ASS-I mainly consists of super refined flocculent particles including amorphous arsenic sulfide adhered with amorphous sulfur and that ASS-II mainly consists of amorphous arsenic sulfide. The valence state of arsenic in both sludges is trivalent, but the valence composition of sulfur is quite different. The ASSs have thermal instability properties. The results of TCLP and CSLT indicate that the concentrations of As and Pd in the leaching solution exceed the standard limits. More than 5% and 90% of arsenic are in the form of acid soluble and oxidizable fractions, respectively, which explains the high arsenic leaching toxicity and environmental activity of ASS. This research provides comprehensive information for the disposal of ASS from copper and lead–zinc smelter.

**Key words:** arsenic sulfide sludge; heavy metals; physicochemical properties; environmental availability; leaching toxicity

### 1 Introduction

Arsenic pollution is widely generated from anthropogenic activities, especially in mining and mineral processing operations [1–3]. The non-ferrous metal extraction process is generally believed to produce large amounts of arsenic-containing acid wastewater [4,5]. In particular, copper or lead–zinc smelting processing produces a large amount of acidic wastewater containing

arsenic and metallic elements [6]. Various treatment processes such as precipitation, adsorption, and biological methods were employed for the removal of arsenic from water [7–9]. To realize the recycling of valuable metals and to minimize the amount of arsenic waste, precipitation by sodium sulfide, sodium hydrosulfide or hydrogen sulphide is one of the most commonly used treatment methods, which generates arsenic sulfide sludge (ASS) [10]. It is estimated that hundreds of thousands of tons of ASS are generated annually in

**Foundation item:** Projects (51904354, 51634010) supported by the National Natural Science Foundation of China; Project (51825403) supported by the National Science Fund for Distinguished Young Scholars, China; Projects (2018YFC1903301, 2018YFC1900301) supported by the National Key R&D Program of China

**Corresponding author:** Yong KE, Tel: +86-731-88830511, Fax: +86-731-88710171, E-mail: [keyong000ke@csu.edu.cn](mailto:keyong000ke@csu.edu.cn);  
Zhang LIN, E-mail: [zhang\\_lin@csu.edu.cn](mailto:zhang_lin@csu.edu.cn)

DOI: 10.1016/S1003-6326(20)65352-3

China; ASS leads to serious environmental pollution risks due to heavy metals leaching in disposal [11].

The physicochemical properties including chemical composition, structural features and mineralogical phase composition directly affect the environmental characteristics and the final disposal methods of the sludge. Our previous studies determined the mineralogy characteristics of zinc leaching residue [12], activity and potential ecological risks of heavy metals in zinc leaching residue [13], the physicochemical and leaching properties of the arsenic-bearing lime–ferrate sludge [14], the release behaviours of arsenic from ASS during simulated storage [11] and the behaviour of arsenic during pyro-metallurgical processing in typical lead smelter [15]. In recent decades, many techniques have been developed to recover heavy metals or arsenic compounds from ASS and to stabilize/solidify harmful elements, including direct extraction [6], roasting [16], crystallization [17,18], vacuum methods [19], hydrothermal methods [20], cement curing [21,22], etc. The choice of recovery or stabilization/solidification (S/S) strongly depends on the sludge characteristics, including the physicochemical and environmental properties. Therefore, in order to find an effective, economical and satisfactory technology, it is necessary to have a detailed and complicated understanding of the characterization of ASS. During the previous decades, some studies have reported the properties of arsenic-containing waste sludge, such as calcium arsenate sludge [14,23,24] and arsenic-bearing iron sludge [25,26]. However, a systematic introduction to the characteristics of ASS has been rarely reported. Some critical technological information on ASS remains unclear, especially for the surface valence distribution of arsenic and sulfur, leaching behaviours, the arsenic phase composition and thermal properties.

The objective of this work was to determine the characteristics of ASS collected from copper and lead–zinc smelter in China, including chemical composition, phase composition, microstructure, thermal properties and leaching toxicity and the relationship between physicochemical properties and arsenic leaching behaviours. This research will introduce reasonable proposals to minimize arsenic leaching concentrations and to provide information

to develop appropriate technologies for the harmless treatment and disposal of this type of sludge.

## 2 Experimental

### 2.1 Materials

The arsenic sulphide sludge used in the experiments was obtained from copper and lead–zinc smelting companies and was named as ASS-I and ASS-II, respectively. The ASSs were precipitated and filtered sludge generated during the treatment of acidic wastewater with sodium sulfide. The collected ASSs were stored and protected from light and oxygen by HDPE film at the companies' hazardous waste yard for several years. The process flow scheme of arsenic production is shown in Fig. 1.

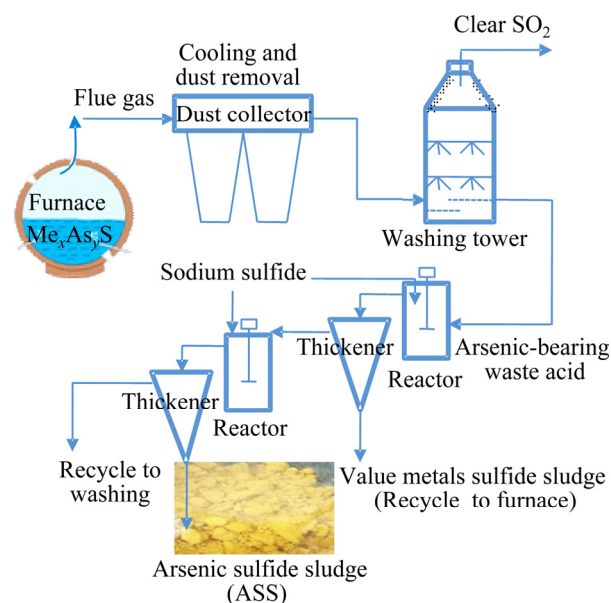


Fig. 1 Flow scheme for ASS production

### 2.2 Leaching tests

#### 2.2.1 Toxicity characteristic leaching procedure (TCLP) and China standard leaching test (CSLT)

The TCLP method is the most commonly used method to evaluate the metal mobility in a sanitary landfill. This test attempts to simulate a worst-case scenario where the waste is co-disposed with municipal solid waste. The detailed procedure of the TCLP tests can be found elsewhere [20]. The CSLT method (GB 5085.3—2007; HJ/T 299—2007) used a mixed solution of sulphuric and nitric acid as

a leaching agent and simulated the process of acid rain leaching of harmful components into the environment. The extraction solution was prepared by the addition of solution (mass ratio of H<sub>2</sub>SO<sub>4</sub> to HNO<sub>3</sub> is 2:1) to adjust the pH (3.20±0.05). The extraction solution was added with a liquid-to-solid ratio of 10:1 (L/kg) [11].

#### 2.2.2 Batch leaching tests

The effects of pH, contact time, temperature and L/S ratio on the leaching behaviours of the arsenic in the ASSs were investigated in the batch leaching experiments. These experiments were performed in batches (250 mL Erlenmeyer) containing 5.0 g of sample and 100 mL of solutions with different pH values (adjusted by diluting a mixture of sulfuric and nitric acids with mass ratio of 3:2). The batches were shaken at 150 r/min using a flask shaker for 24 h. The final filtrates were acidified and analyzed.

#### 2.2.3 Multiple extraction procedure (MEP)

The MEP (USEPA, 1986) method simulated leaching conditions that occurred when a waste undergoes repetitive acid rain on an improperly designed sanitary landfill. It is commonly used to estimate the potential long-term leachability of contaminants from solid wastes [27]. In the first step, the waste sample was extracted with acetic acid solution at an L/S ratio of 20:1 for 24 h. The suspension pH was maintained at 5 by the addition of 0.5 mol/L acetic acid during the extraction. The residual solids after the extraction were consecutively re-extracted four times using synthetic acid rain extraction fluid with pH 3.0±0.2, which was a dilute mixture of sulfuric and nitric acids with mass ratio of 3:2 (or a suitable dilution). Each extraction step was performed at L/S ratio of 20:1 for 24 h. The final metal ion concentrations were determined for each extraction.

#### 2.2.4 Sequential extraction scheme

A three-step extraction procedure was proposed by the Community Bureau of Reference (BCR). In this work, Davidson's three-stage BCR sequential extraction procedure was used to analyze the effective combination forms of heavy metals in the sludges. The detailed procedure of the BCR tests can be found elsewhere [13].

### 2.3 Analysis

#### 2.3.1 Determination of elemental composition

The contents of heavy metals such as As, Cd,

Cr, Pb, Cu and Zn in the raw material were determined using ICP-OES (Agilent 5100). Prior to the ICP-OES tests, the sample was digested through microwave- assisted acid digestion according to the procedure described in our previous study [28].

#### 2.3.2 Determination of phase composition

The arsenic-containing compound was analyzed by a chemical phase analysis method to obtain the phase composition of arsenic in the sludge [11]. The arsenic phases were obtained by extraction and separation of different reagents.

#### 2.3.3 X-ray photoelectron spectroscopy (XPS)

X-ray photoelectron spectroscopy (XPS) measurements were carried out on a Thermo Fisher Scientific ESCALAB 250Xi using Al K<sub>α</sub> X-ray as the excitation source. The base pressure in the analysis chamber was 133.3×10<sup>-9</sup> Pa. Peak shifts due to surface charging were taken into account by normalizing energies based on the adventitious carbon peak at 284.5 eV. Survey and narrow-scan XPS spectra were obtained using pass energies of 100 and 30 eV, respectively. Survey scans were used to determine the average composition of the surface. The semi-quantitative composition of the near-surface samples was calculated from the peak areas of the S 2p and As 3d peaks and normalized by their respective sensitivity factor [29]. Narrow-scan spectra were obtained in order to determine the S and As surface species.

#### 2.3.4 Others analysis

The crystallographic composition of the samples was characterized by X-ray diffraction (XRD, D/max2550VB+18 kW) with steps of 0.02° at 10 (°)/min in a 2θ range from 10° to 80°. The morphological change of the samples was observed with a scanning electron microscope (SEM-EDS, Nova NanoSEM 230, Brno, Czech Republic). Thermal stability of sludges are evaluated by TG-DTA test (a STA 449 F3 A-0488M instrument in flowing argon at a heating rate of 10 °C/min). Raman spectra (LABRAM-HR 800 spectrometer, Renishaw inVia, Gloucestershire, UK) were recorded with a 513 nm-wavelength He-Ne laser and an acquisition time of 10 s.

## 3 Results and discussion

### 3.1 Physicochemical properties

#### 3.1.1 Chemical compositions of ASSs

The chemical compositions of ASSs are given

in Table 1. ASS-I contains S (50.4%) and As (35.1%) as the major elements. Varying amounts of other minor elements such as Cu (0.36%) and Na (0.34%) also occur in the ASS-I. The contents of Pb, Zn and Cd in the sludge are very low (less than 0.1%). The major elements of ASS-II are also As (43.7%) and S (30.9%). The content of As is significantly higher than that of ASS-I. The contents of other minor elements such as Cd (4.14%), Pb (0.23%), Zn (0.725%), Sb (2.13%), Fe (0.67%) and K (0.143%) are also higher than those of ASS-I. From this result, it was found that the pollutant elemental content of ASS from lead–zinc smelter is significantly higher than that of copper smelter. The chemical compositions are essentially consistent with our previous studies and other related studies [6,11,19,20].

### 3.1.2 Phase and chemical speciation of arsenic

The chemical composition results show that the sludge is mainly composed of S and As, indicating that the particles may be As–S compounds. The XRD patterns (Fig. 2) of the two sludges exhibit weak and broad diffraction peaks, confirming that they are mostly non-crystalline. The three broad peaks occur at  $2\theta$  values near  $18^\circ$ ,  $31^\circ$  and  $57^\circ$ , similar to amorphous  $\text{As}_2\text{S}_3$  [11,20,30–32]. The CdS crystal structures are found in ASS-II. The Raman technique is further applied to investigating the structure of ASSs. In

ASS-I, four peaks located at  $\sim 153$ ,  $\sim 218$ ,  $\sim 340$ , and  $\sim 473 \text{ cm}^{-1}$  are found from Fig. 2. The peak at  $\sim 340 \text{ cm}^{-1}$  indicates the existence of  $\text{As}_2\text{S}_3$ , while the others ( $\sim 153$ ,  $\sim 218$ , and  $\sim 473 \text{ cm}^{-1}$ ) suggest the presence of S [20], which means that there may be some amorphous sulfur in the ASS-I when combined with the XRD patterns and chemical composition results. However, there is one distinct peak of  $\sim 340 \text{ cm}^{-1}$  in ASS-II, indicating that there is  $\text{As}_2\text{S}_3$  in the sludge and less elemental S.

Table 2 also shows the phase compositions of arsenic which were analyzed by a chemical phase analysis method. The result indicates that 18.07% and 20.93% of the arsenic exist in the form of arsenic oxides, compared with 80.94% and 77.41% in the form of As–S compounds for ASS-I and ASS-II, respectively. It is obvious that arsenic is mainly in the sulfide state, but the oxidized state cannot be ignored and its impact on environmental properties is critical. In our previous study, the oxide phase compositions of the arsenic were 79.9% for the Cu–As-containing filter cake [6] and 49.56% for the ASS from a copper smelting plant in Yunnan Province, China [11]. This difference is possibly attributed to the oxidation of arsenic sulfide during the storage period and drying process. Our previous study showed that the ASS would be oxidized to  $\text{As}_2\text{O}_3$  in the presence of oxygen or oxygen-free during the storage process [11].

**Table 1** Main elemental compositions of ASSs (wt. %)

Sludge	As	Cd	Pb	Cr	Hg	Cu	Zn	Sb	Fe	Na	K	S
ASS-I	35.1	0.001	0.08	<0.001	0.029	0.36	<0.001	0.03	0.02	0.34	0.006	50.4
ASS-II	43.7	4.14	0.23	0.06	0.015	0.02	0.725	2.13	0.67	0.37	0.143	30.9

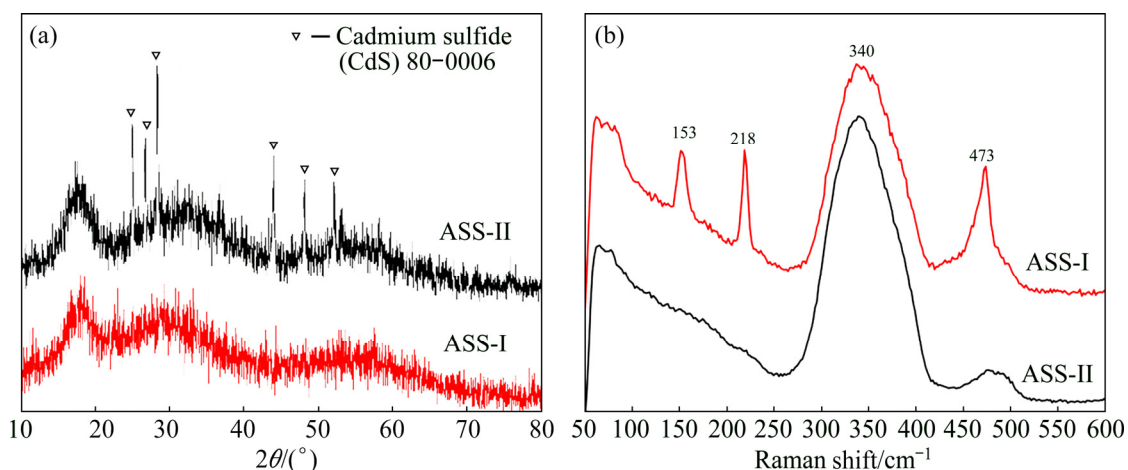


**Fig. 2** XRD patterns (a) and Raman spectra (b) of ASSs

**Table 2** Arsenic phase composition of ASSs obtained by chemical analysis method

Composition	Mass fraction/%	
	ASS-I	ASS-II
Arsenic oxides	18.07	20.93
Arsenate & arsenite	0.01	0.02
Arsenic sulfide	80.94	77.41
Others	0.98	1.64
Total	100	100

### 3.1.3 Morphological and particle size features

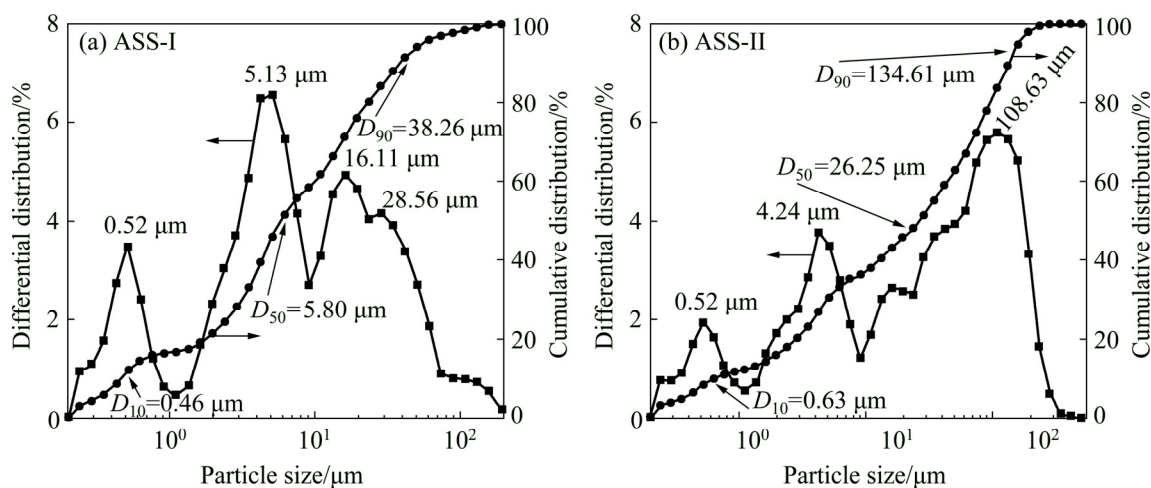
Figure 3 shows a wide range of the particle size distribution from 0.2 to 500  $\mu\text{m}$ . The size of the ASS-I particles is distributed in four concentrated areas of approximately 0.52, 5.13, 16.11 and 28.56  $\mu\text{m}$ . The median particle size ( $D_{50}$ ) of 5.80  $\mu\text{m}$  indirectly reflects that most small particles are adhered into large particles. However, the agglomeration of particles in the ASS-II sludge is more pronounced. The size of the ASS-II particles is distributed in three concentrated areas of approximately 0.52, 4.24 and 108.63  $\mu\text{m}$ . The median particle size ( $D_{50}$ ) of 26.25  $\mu\text{m}$  indirectly reflects that most small particles are agglomerated into larger particles. The particle agglomeration of the ASS-II is more obvious than that of ASS-I. In the arsenic-bearing water treatment process, the dosing of PAM (polyacrylamide) has an important influence on the agglomeration of the particles.

The morphological features play an important role for the environmental characteristics and treatments of solid waste. Figure 4 shows the morphology of the two sludges, and it is clear that

there is a significant difference between the two granules. As seen in Figs. 4(a, b, c), the large particles are adhered and aggregated by irregularly sized particles of various sizes. It can be seen that some amorphous tiny particles are adsorbed on the surface of big irregular bulk shaped substances. Combined with the XRD, EDS and Raman results, the tiny particles that are adsorbed on the outer layer may be  $\text{As}_2\text{S}_3$ , and the large internal substance may be elemental S. It can be seen from Figs. 4(d–f) that the particles in the sludge are very fine, the size of the particles is relatively uniform and the amorphous tiny particles agglomerate into large particles. Compared with ASS-I, granulation is not obvious as there is no phenomenon of large and small particles being wrapped, and the overall shape is fluffy and cotton-like. The S particles generated in an irradiated  $\text{As}_2\text{S}_3$  system can efficiently coalesce into  $\text{As}_2\text{S}_3$  particles and the formation of  $[\text{As}_2\text{S}_2\text{-S-S-S}_2\text{As}_2]^{2+}$  results in the aggregation of the sulfide particles [32]. The presence of S has an important influence on the particle morphology and particle characteristics.

### 3.1.4 Surface composition of arsenic and sulfur

XPS survey-spectra of the ASSs are shown in Fig. 5(a). These data indicate the presence of S, As and O. It can be seen that the intensity of peak As 3d for ASS-I is lower than that of ASS-II, but the peak of S 2p is higher. Table 3 shows the atom ratio of the As and S species by XPS survey-spectra. The atom ratios of S and As species are 69:31 for ASS-I, and 62:38 for ASS-II, respectively. The content of S in ASS-I is obviously higher than that in ASS-II. The result is basically consistent with the conclusions of Raman (Fig. 2) and EDS (Fig. 5(b)).

**Fig. 3** Particle size distribution of ASS-I (a) and ASS-II (b)

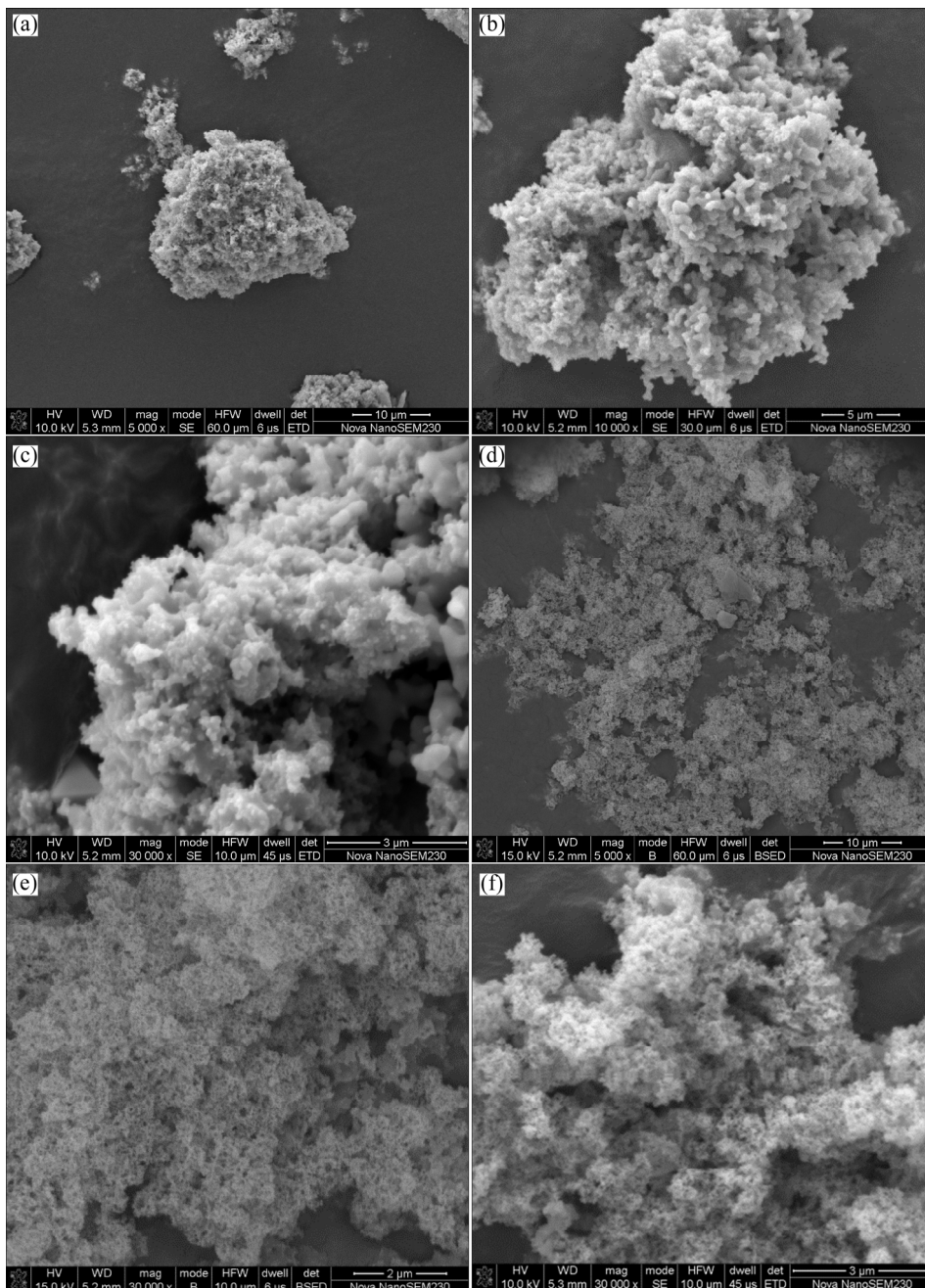


Fig. 4 SEM images of ASS-I (a, b, c) and ASS-II (d, e, f)

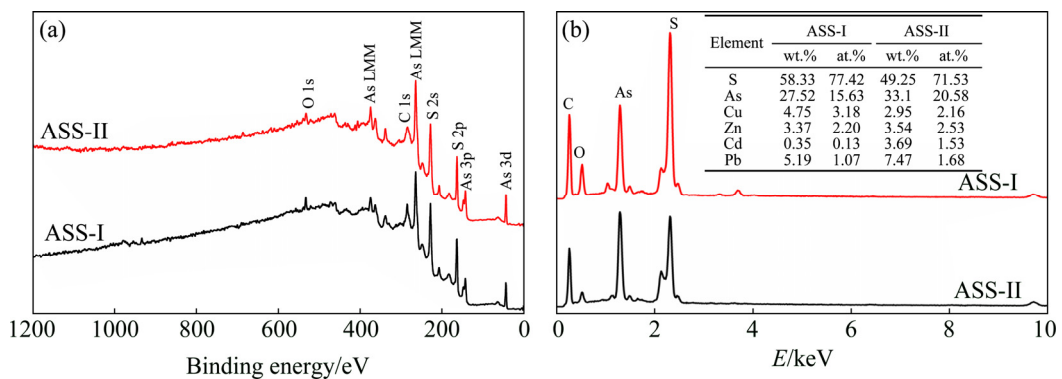


Fig. 5 XPS spectra at high pass energy of 100 eV (a) and EDS analysis (b) of ASSs

The elemental spectra are fitted using a least-squares procedure with peaks of convoluted Gaussian (80%) and Lorentzian (20%) peak shape after subtraction of a Shirley baseline. The As 3d spectra are modelled as doublets of  $3d_{3/2}$  and  $3d_{5/2}$ , separated by 0.7 eV. The area of the As  $3d_{3/2}$  peak is two-thirds that of the As  $3d_{5/2}$  peak. The peaks of As  $3d_{5/2}$  at 43.4 eV are attributed to As(III)—S. The major peaks of S 2p spectra contain peaks at 162.7, 163.7 and 164.7 eV for ASS, which are assigned to monosulfide ( $S^{2-}$ ), disulfide ( $S_2^{2-}$ ) and sulphur ( $S^0$ ). According to Table 3 and Fig. 6, the binding energy of the As  $3d_{5/2}$  peaks is fitted with one As

component of As(III). This phenomenon is consistent with the results of Raman analysis. As shown in Table 3, the component of As(III) predominates the As speciation and reaches 100%. As(V) and As(II) are not found to be related to the redox characteristics of the sulfurization reaction process. It has been reported that As(V) is first reduced to As(III) by sulfur ions, and then  $As_2S_3$  is precipitated [30]. Since As(III) and S can form precipitates rapidly, it is less likely that As would continue to be reduced to As(II) under normal conditions to form  $As_4S_4$ . It is clear that the contents of  $S^0$  and  $S_2^{2-}$  for ASS-I are 7% and 4% higher than

**Table 3** Analysis results of XPS spectra of As 3d and S 2p for ASSs

Sample		As 3d	S 2p	As(III)	$S^0$	$S_2^{2-}$	$S^{2-}$
ASS-I	$E_b/eV$	43.7(1.40)	163.6(2.18)	43.49(0.93)	164.82(1.08)	163.77(1.08)	162.77(0.98)
	Percent/%	31	69	100	17	50	33
ASS-II	$E_b/eV$	43.75(1.41)	163.04(2.27)	43.54(0.91)	164.63(1.26)	163.73(1.17)	162.650(0.99)
	Percent/%	38	62	100	10	46	44

$E_b$ : Binding energy (FWHM)

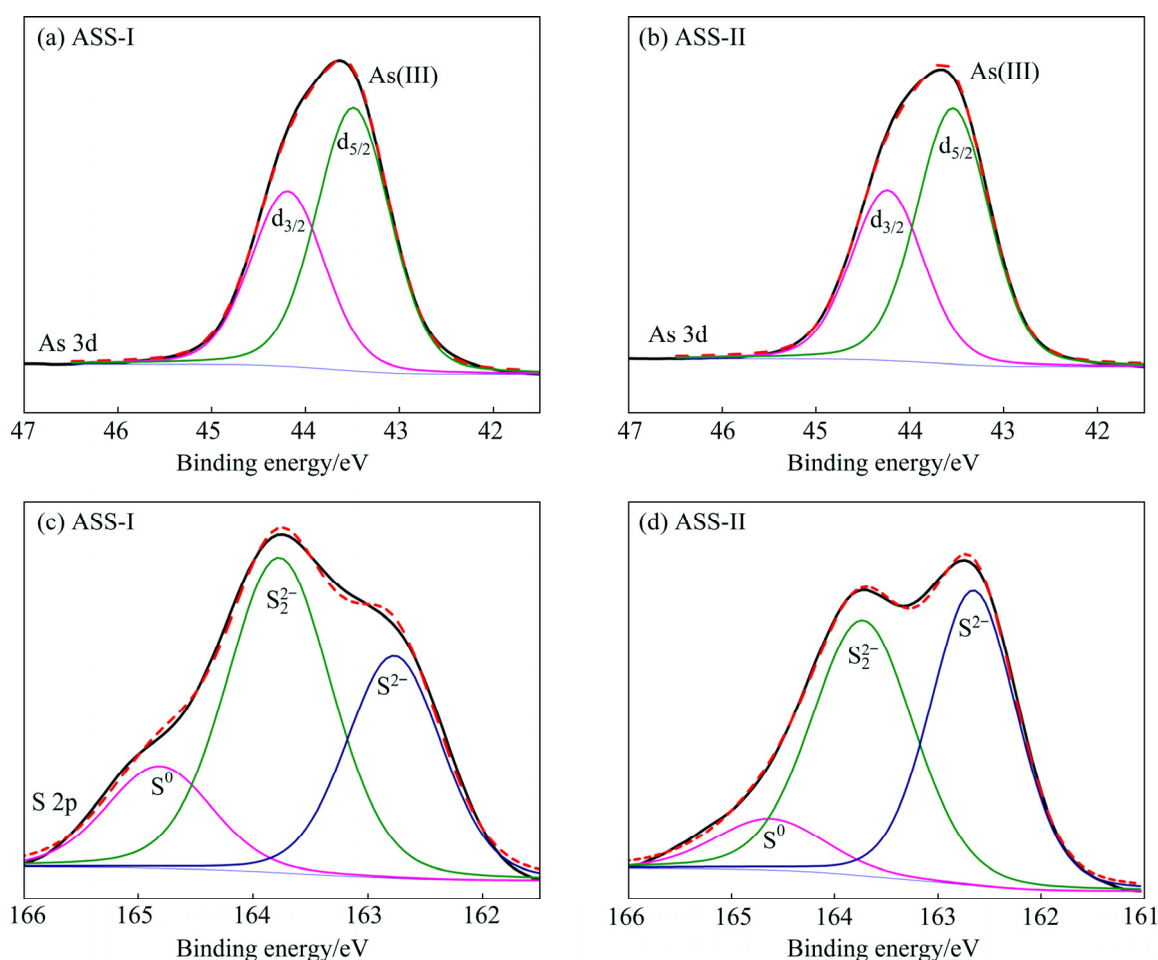


**Fig. 6** XPS spectra of As 3d (a, b) and S 2p (c, d) peaks for ASSs at low pass energy of 30 eV

those for ASS-II, respectively. However, the  $S^{2-}$  for ASS-I is 11% lower than that of ASS-II. The difference may be related to the valence state of arsenic in the acidic arsenic-containing wastewater and the redox characteristics of the solution before the sulfide precipitation.

### 3.1.5 Thermal characteristics

TG–DTA is performed to confirm the thermal stability of the sludge, and the TG–DTG–DSC curves of the ASSs are shown in Fig. 7. As shown in Fig. 6, two broad and four sharp mass loss stages are observed for ASS-I. In the first stage (step 1), a heavy mass loss of 6% is observed from approximately 50 to 150 °C. This is attributed to the volatilization of adsorbed and bounded water. The DTG also reflects the dehydration peak in the temperature range. In the next stage at 150–225 °C (step 2), a heavy mass loss of 7% is ascribed to the oxidization of  $As_2S_3$  and S to  $SO_2$  by concentrated sulfuric acid. The phenomenon was also observed in our research [11]. The acid may attack metal-bearing phases and promote further exposure of other sulfides encapsulated [33,34]. The next sharp peaks may be caused by the volatilization of S and

sulfide. However, one broad mass loss stage is found for ASS-II, and the mass loss is obviously accelerated after 225 °C. The first stage from 50 to 150 °C is similar to ASS-I; a heavy mass loss of 1.4% due to volatilization of adsorbed and bounded water. In the next stage of 150–225 °C, the heavy mass loss is 0.9%. The mass loss after 250 °C may be the result of volatilization of sulfides. The thermal stability of ASS-I is significantly worse than ASS-II. The presence of sulfuric acid and elemental S may have a significant effect on the thermal stability of the ASSs.

## 3.2 Environmental properties

### 3.2.1 Leaching behaviours

The release of pollutants in solid waste can be affected by changes of landfill and storage conditions. The effects of pH, contact time, liquid/solid ratio and temperature on the dissolution of As in the ASSs were investigated. The results are presented in Fig. 8. Figure 8(a) shows that the leaching concentration of As decreased rapidly and then slowly with the increase of L/S ratio. With the variation of pH, the change trends of As leaching concentration for the two ASSs are similar (Fig. 8(b)). The As leaching concentrations of ASS-I and ASS-II first increase and then decrease. Although the pH of the extract liquor is continuously increased to 13, the leached solution is still acidic (pH<3) after the leaching test because the sludge contained a bit of sulfuric acid solution. The leaching of heavy metals in many copper slags has a strong relationship with pH, but the sulphides are the least stable phases regardless of conditions [35]. As shown in Fig. 8(c), the effect of leaching time on leaching concentration of As is significant. With the extension of time, the leaching concentration of As increases rapidly and remains stable for ASS-I, whereas the leaching concentration of As for ASS-II increase rapidly in the entire time range investigated. Temperature has a great influences on the leaching concentration of As (Fig. 8(d)). When the temperature is increased from 15 to 20 °C, the As leaching concentrations of ASS-I and ASS-II increase from 112 mg/L (2.24 mg/kg, 0.64%) to 808 mg/L (16.16 mg/kg, 4.60%) and from 531 mg/L (10.62 mg/kg, 2.43%) to 1422 mg/L (28.44 mg/kg, 6.51%), respectively. As the temperature increases from 20 to 30 °C, the As leaching concentration increases slowly. The

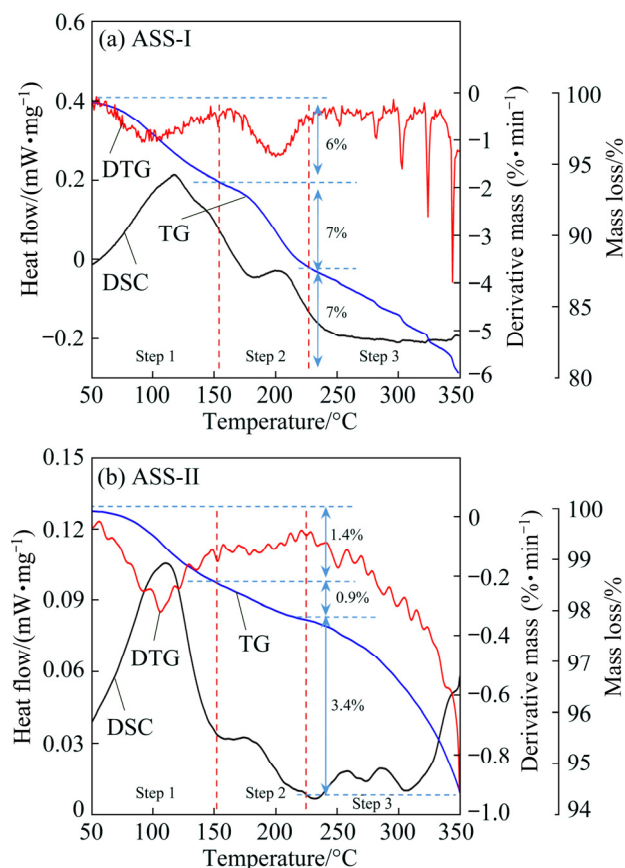


**Fig. 7** TG–DTG–DSC curves of ASS-I (a) and ASS-II (b)

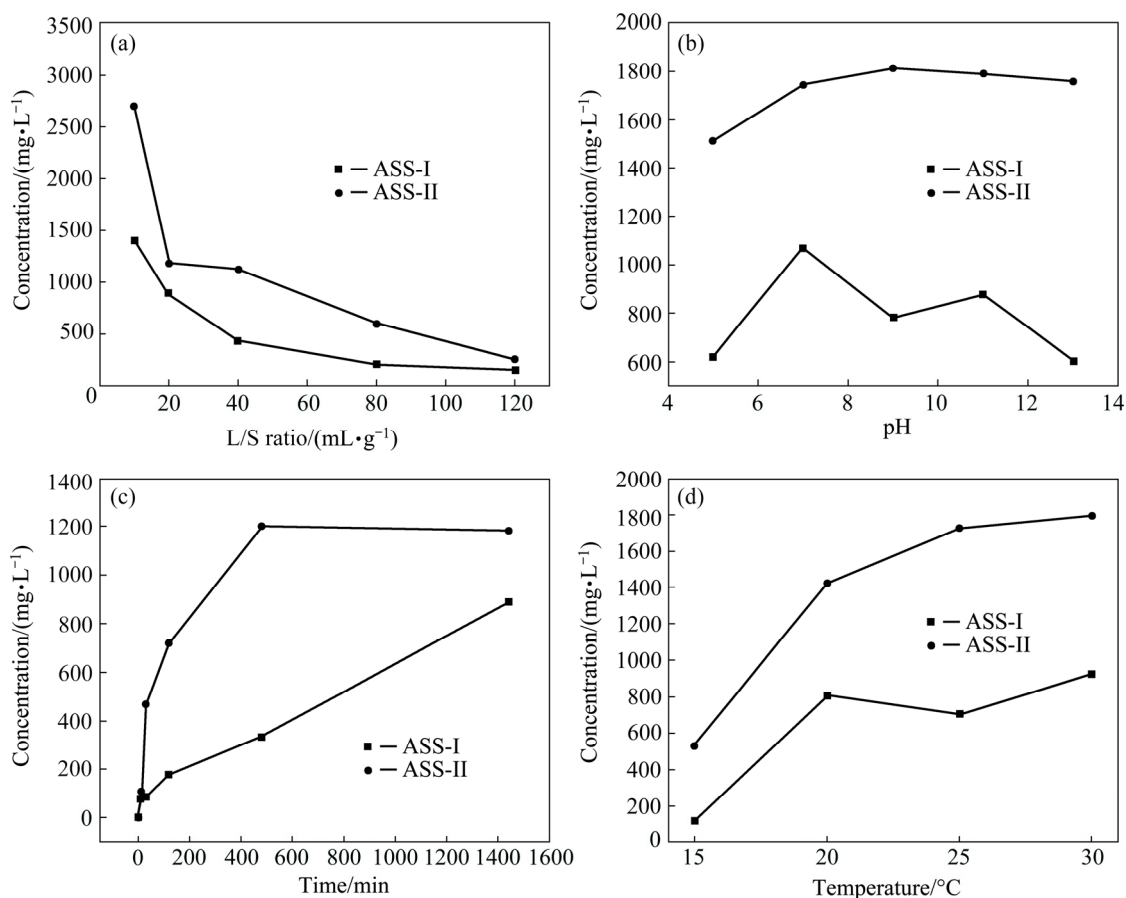


Fig. 8 Effects of leaching factors on concentration of arsenic

ASSs are sensitive to external factors, probably due to the strong interfacial interaction of the amorphous nano-particles.

### 3.2.2 Leaching toxicity

To determine whether the sample can be disposed in a segregated landfill, TCLP and CSLT tests are employed on the ASSs. The results are presented in Table 4. TCLP and CSLT test results show that both concentrations of As and Pb released from ASS-I exceed the threshold values of US Environmental Protection Agency (EPA) and GB 5085.3—2007. The arsenic concentration of ASS-I exceeded the EPA standard by 52 times and GB 5085.3—2007 by 268 times. The concentrations of As, Pb and Cd dissolved from the ASS-II exceeded the threshold values of the EPA and GB 5085.3—2007. The concentration of Zn exceeded the threshold value of GB 5085.3—2007 and the Cd concentration seriously exceeded the standard for ASS-II. The ASSs must be considered hazardous pollutants and cannot be discharged with domestic waste unless they are stabilized and solidified.

Table 4 Leaching concentrations of raw ASSs (mg/L)

Sample	Method	As	Pb	Zn	Cu	Cd	Cr
ASS-I	TCLP	261.0	12.90	4.5	1.20	0.6	0.05
	CSLT	1344.5	1.23	7.8	0.25	2.1	0.13
ASS-II	TCLP	780.0	7.70	350.0	0.05	917.0	7.12
	CSLT	1297.5	11.63	917.5	0.20	3226.0	18.50
EPA <sup>#</sup>		≤5	≤5	<sup>b</sup>	<sup>b</sup>	≤1	≤5
GB 5085.3—2007 <sup>*</sup>		≤5	≤1.0	≤100	≤100	≤5	<sup>b</sup>

<sup>\*</sup>The threshold of China; <sup>#</sup> The threshold of the US; <sup>b</sup> Not limited in the standard

### 3.2.3 Sustainable leaching properties

Figure 9 shows the results of multiple extraction procedure (MEP). The first extraction of the MEP was performed using leaching fluid with pH 2.88 adjusted by adding 0.5 mol/L acetic acid. The subsequent extractions were performed using pH 3.0±0.2 synthetic rainwater. During the first two leaching processes, the concentrations of As and heavy metals decrease rapidly, and the decreased trends slowly become significant in the next three leaching processes. The results show a relatively

high residual As concentration (>5 mg/L) for the ASSs at the end of the test. According to the MEP results, it can be concluded that ASS is a solid waste with sustainable pollution potential. Similar results were found by ÖZVERDİ and ERDEM [27], showing that the Zn, Mn and Cd concentrations decreased rapidly and then slowly with the consecutive extractions for zinc extraction residue.

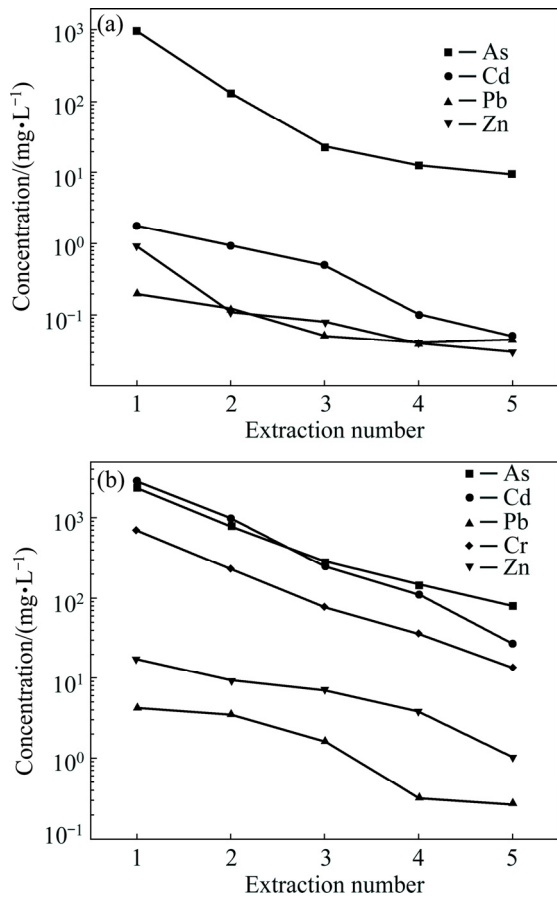


Fig. 9 Effect of extraction number on concentrations of heavy metals: (a) ASS-I; (b) ASS-II

### 3.2.4 Environmental activity

Study of the chemical special speciation of the arsenic and heavy metals for the sludge is important for analyzing environmental activity. The species from sequence extraction could yield the chemical forms, physicochemical availability, and mobilization of trace metals. Generally, arsenic and other heavy metals in the acid soluble fraction are classified as direct effect phases for environmental availability and ecological risk. The oxidizable fraction is identified as a potential effect fraction because it can be liberated or transformed into an acid soluble fraction under oxidizing conditions [11].

It can be seen from Fig. 10 that the acid soluble and oxidizable states of As and heavy metals are dominant. For ASS-I, the oxidizable states are dominant, and the oxidizable states of As, Pb, Zn, Cu, Cd and Cr are 94.7%, 98.9%, 98%, 100%, 99.9% and 99.9%, respectively. The acid soluble states are 5.0%, 0.8%, 1.4%, 0.0%, 0.1% and 0.1%, respectively. For ASS-II, the acid soluble states of Zn and Cr are dominant. The oxidizable forms of As, Pb, Zn, Cu, Cd and Cr are 91.9%, 96.5%, 25.3%, 66.6%, 69.6% and 1.3%, respectively. Their acid soluble states are 7.2%, 2.4%, 74.6%, 33.3%, 30.4% and 98.7%, respectively. The water soluble phase and exchangeable phase heavy metals will be easily released in an acid rain environment. The results show that As and Pb for the two ASSs have high environmental activity and can be easily and quickly released into the environment. The acid soluble states of ASS-II are more than those of

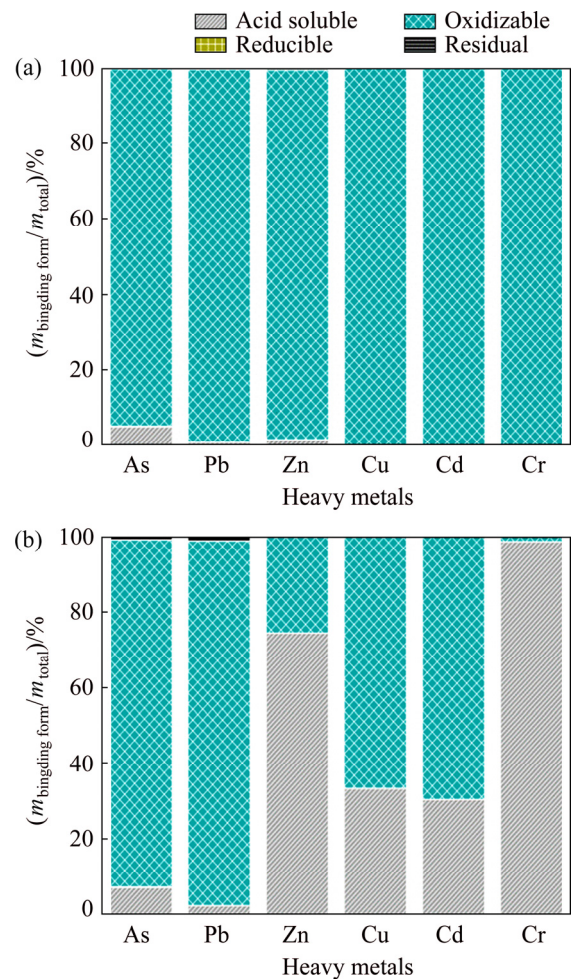


Fig. 10 Chemical fractions of heavy metals species in ASSs by BCR sequential extraction procedure: (a) ASS-I; (b) ASS-II

ASS-I, meaning that the risk of ASS-II is higher than that of ASS-I. The oxidizable forms of heavy metals mostly bound to sulfides can be easily released under oxidized conditions. This reveals that the sulfides of As and other heavy metals would be oxidized and released in an oxidizing environment and over along the time.

### 3.3 Recommendation for appropriate disposal

According to the studies above, it is clear that the leaching behaviours of arsenic and heavy metals in the ASSs are mainly related to their properties and that the phase composition is determined in the sulfuration treatment process of arsenic-containing wastewater and is reliant on storage conditions. It is beneficial to the long-term stability of residues in the form of arsenic combined with calcium, iron or aluminium [36,37]. Arsenic, mainly in the presence of amorphous arsenic sulfide and arsenic oxide phase, occupies 80.94%–77.41% and 18.07%–20.93%, respectively. This is the main cause of the high arsenic leaching toxicity and environmental risk of ASSs and the potential long-term environmental risk under oxidizing conditions. Arsenic in the ASS is all trivalent arsenic according to the XPS analysis. Since the toxicity of trivalent arsenic is 60 times that of pentavalent arsenic [38], the damage of the ASS is generally higher than that of calcium arsenate and iron arsenate sludge.

Developing effective harmless disposal methods for ASS is an urgent requirement. Based on the high toxicity, poor stability, and ease of oxidation for acid flocculous ASS, stabilization by phase transformation may be a suitable method. ASS can be converted into a relatively stable calcium arsenate or iron arsenate by oxidative leaching, precipitation and crystallization. However, it requires a large amount of oxidant and stabilization agent, and a significant increase in mass and volume after conversion. The presence of sulfur would interfere with the conversion effect. The conversion of amorphous arsenic sulfide to crystalline  $As_2S_3$  or  $As_4S_4$  may be the best solution. However, there are currently few studies on this, probably because of the harsh conditions and high energy consumption. Our research finds that hydrothermal treatment of arsenic sulfide is a feasible technical means, but there are still many problems to be further studied and solved. It is necessary and useful to analyze the

physicochemical properties and environmental characteristics to discover novel stabilization techniques.

## 4 Conclusions

(1) ASS-I is mainly composed of amorphous  $As_2S_3$  and amorphous S, while ASS-II is mainly composed of amorphous  $As_2S_3$  and crystal CdS. Many small particles (amorphous  $As_2S_3$ ) are adhered into large particles (amorphous S) for ASS-I.

(2) Arsenic phases exist as As(III) mainly in sulfides (80.94%–77.41%) and oxides (18.07%–20.93%), and disperse uniformly in amorphous particles. More sulfur species of  $S^0$  and  $S_2^{2-}$  are observed on the surface of ASS-I than that of ASS-II. Both ASSs are thermally instable and can easily be decomposed or lose mass. The thermal stability of ASS-I is worse than ASS-II.

(3) Both TCLP and CSLT assessment methods identified that the ASSs could be classified as hazardous solid waste by the EPA or Chinese government. The leachate concentration of As and Pb in the two ASSs exceeded the standard, and Cd in ASS-II seriously exceeded the standard.

(4) MEP showed that the ASSs have sustainable release characteristics and still exceeded the standard limits after five leaching cycles. From the BCR sequential extraction results, the oxidable states of As, Pb, Cu and Cd are dominant for the ASSs, but the acid soluble states of Zn and Cr are dominant for ASS-II.

(5) Crystallization of arsenic phases in ASS should be beneficial to decreasing arsenic leaching toxicity and thus reducing environmental risk.

## References

- [1] AM S D L C, SÁNCHEZ-RODAS D, GONZÁLEZ C Y, JD D L R. Geochemical anomalies of toxic elements and arsenic speciation in airborne particles from Cu mining and smelting activities: influence on air quality [J]. *Journal of Hazardous Materials*, 2015, 291: 18–27.
- [2] CHAI L Y, YANG J Q, ZHANG N, WU P J, LI Q Z, WANG Q W, LIU H, YI H B. Structure and spectroscopic study of aqueous Fe(III)–As(V) complexes using UV–Vis, XAS and DFT-TDDFT [J]. *Chemosphere*, 2017, 182: 595–604.
- [3] FEI J C, WANG T, ZHOU Y Y, WANG Z X, MIN X B, KE Y, HU W Y, CHAI L Y. Aromatic organo-arsenic compounds (ADCs) occurrence and remediation methods [J]. *Chemosphere*, 2018, 207: 665–675.

- [4] FEI J C, MIN X B, WANG Z X, PANG Z H, LIANG Y J, KE Y. Health and ecological risk assessment of heavy metals pollution in an antimony mining region: A case study from South China [J]. *Environmental Science & Pollution Research*, 2017, 24(35): 27573–27586.
- [5] LUO T, CUI J L, HU S, HUANG Y Y, JING C Y. Arsenic removal and recovery from copper smelting wastewater using TiO<sub>2</sub> [J]. *Environmental Science & Technology*, 2010, 44(23): 9094–9098.
- [6] KE Y, SHEN C, MIN X B, SHI M Q, CHAI L Y. Separation of Cu and As in Cu–As-containing filter cakes by Cu<sup>2+</sup>-assisted acid leaching [J]. *Hydrometallurgy*, 2017, 172: 45–50.
- [7] ANDJELKOVIC I, JOVIC B, JOVIC M, MARKOVIC M, STANKOVIC D, MANOJLOVIC D, ROGLIC G M. Microwave-hydrothermal method for the synthesis of composite materials for removal of arsenic from water [J]. *Environmental Science & Pollution Research*, 2016, 23(1): 469–476.
- [8] MIN X B, LI Y, KE Y, SHI M Q, CHAI L Y, XUE K. Fe–FeS<sub>2</sub> adsorbent prepared with iron powder and pyrite by facile ball milling and its application for arsenic removal [J]. *Water Science & Technology*, 2017, 76(1): 192–200.
- [9] CHAI L Y, YUE M Q, YANG J Q, WANG Q W, LI Q Z, LIU H. Formation of tooeite and the role of direct removal of As(III) from high-arsenic acid wastewater [J]. *Journal of Hazardous Materials*, 2016, 320: 620–627.
- [10] BAI M, ZHENG Y J, LIU W Y, ZHANG C F. Alkaline leaching and leaching kinetics of arsenic sulfide residue [J]. *Journal of Central South University (Science and Technology)*, 2008, 39(2): 268–272. (in Chinese)
- [11] YAO L W, MIN X B, KE Y, WANG Y Y, LIANG Y J, YAN X, XU H, FEI J C, LI Y C, LIU D G, YANG K. Release behaviors of arsenic and heavy metals from arsenic sulfide sludge during simulated storage [J]. *Minerals*, 2019, 9(130): 1–16.
- [12] LI M, PENG B, CHAI L Y, PENG N, XIE X D, YAN H. Technological mineralogy and environmental activity of zinc leaching residue from zinc hydrometallurgical process [J]. *Transactions of Nonferrous Metals Society of China*, 2013, 23(5): 1480–1488.
- [13] MIN X B, XIE X D, CHAI L Y, LIANG Y J, LI M, KE Y. Environmental availability and ecological risk assessment of heavy metals in zinc leaching residue [J]. *Transactions of Nonferrous Metals Society of China*, 2013, 23(1): 208–218.
- [14] PENG B, LEI J, MIN X B, CHAI L Y, LIANG Y J, YOU Y. Physicochemical properties of arsenic-bearing lime-ferrate sludge and its leaching behaviors [J]. *Transactions of Nonferrous Metals Society of China*, 2017, 27(5): 1188–1198.
- [15] CHAI L Y, SHI M Q, LIANG Y J, TANG J W, LI Q Z. Behavior, distribution and environmental influence of arsenic in a typical lead smelter [J]. *Journal of Central South University*, 2015, 22(4): 1276–1286.
- [16] NAZARI A M, RADZINSKI R, GHAHREMAN A. Review of arsenic metallurgy: Treatment of arsenical minerals and the immobilization of arsenic [J]. *Hydrometallurgy*, 2017, 174: 258–281.
- [17] CERNOSEK Z, CERNOSKOVA E, BENES L. Crystalline arsenic trisulfide: Preparation, differential scanning calorimetry and Raman scattering measurements [J]. *Mater Letters*, 1999, 38(5): 336–340.
- [18] MA X, GOMEZ M A, YUAN Z D, ZHANG G Q, WANG S F, LI S F, YAO S H, WANG X, JIA Y F. A novel method for preparing an As(V) solution for scorodite synthesis from an arsenic sulphide residue in a Pb refinery [J]. *Hydrometallurgy*, 2019, 183: 1–8.
- [19] HU H J, QIU K Q. Three-step vacuum separation for treating arsenic sulphide residue [J]. *Vacuum*, 2015, 111: 170–175.
- [20] YAO L W, MIN X B, XU H, KE Y, LIANG Y J, YANG K. Hydrothermal treatment of arsenic sulfide residues from arsenic-bearing acid wastewater [J]. *International Journal of Environmental Research and Public Health*, 2018, 15(9): 1–15.
- [21] ZHOU S, SHANG T, ZHONG P, LIU W. Stabilization and solidification of strong acidic arsenic sulfide residue [J]. *Environmental Protection of Chemical Industry*, 2015, 35(5): 513–515. (in Chinese)
- [22] DU Y, XIAO H, LU Q, DU D. Using manganese slag to stabilize/solidify arsenic sulfide slag by moderate temperature calcinations [J]. *Chinese Journal of Environmental Engineering*, 2017, 11(2): 1136–1140. (in Chinese)
- [23] LI X, ZHU X, QI X J, LI K Z, WEI Y G, WANG H, HU J H, HUI X H, ZHANG X. Pyrolysis of arsenic-bearing gypsum sludge being substituted for calcium flux in smelting process [J]. *Journal of Analytical & Applied Pyrolysis*, 2018, 130: 19–28.
- [24] LEI J, PENG B, MIN X B, LIANG Y J, YOU Y, CHAI L Y. Modeling and optimization of lime-based stabilization in high alkaline arsenic-bearing sludges with a central composite design [J]. *Journal of Environmental Science and Health: Part A*, 2017, 52(5): 449–458.
- [25] ROY A, van GENUCHTEN C M, MOOKHERJE I, DEBSARKAR A, DUTTA A. Concrete stabilization of arsenic-bearing iron sludge generated from an electrochemical arsenic remediation plant [J]. *Journal of Environmental Management*, 2019, 233: 141–150.
- [26] MAJZLAN J, DACHS E, BENISEK A, DRAHOTA P. Thermodynamic properties of FeAsO<sub>4</sub>·0.75H<sub>2</sub>O—A more favorable disposable product of low As solubility [J]. *Hydrometallurgy*, 2016, 164: 136–140.
- [27] ÖZVERDİ A, ERDEM M. Environmental risk assessment and stabilization/solidification of zinc extraction residue: I. Environmental risk assessment [J]. *Hydrometallurgy*, 2010, 100(3–4): 103–109.
- [28] KE Y, CHAI LY, MIN X B, TANG C J, CHEN J, WANG Y, LIANG Y J. Sulfidation of heavy-metal-containing neutralization sludge using zinc leaching residue as the sulfur source for metal recovery and stabilization [J]. *Minerals Engineering*, 2014, 61: 105–112.
- [29] RENOCK D, GALLEGOS T, UTSUNOMIYA S, HAYES K, EWING R C, BECKER U. Chemical and structural characterization of As immobilization by nanoparticles of mackinawite (FeSm) [J]. *Chemical Geology*, 2009, 268(1–2): 116–125.
- [30] KONG L H, PENG X J, HU X Y. Mechanisms of UV-light

- promoted removal of As(V) by sulfide from strongly acidic wastewater [J]. *Environmental Science & Technology*, 2017, 51(21): 12583–12591.
- [31] PENG X J, CHEN J Y, KONG L H, HU X Y. Removal of arsenic from strongly acidic wastewater using phosphorus pentasulfide as precipitant: UV-light promoted sulfuration reaction and particle aggregation [J]. *Environmental Science & Technology*, 2018, 52(8): 4794–4801.
- [32] KONG L H, PENG X J, HU X Y, CHEN J Y, XIA Z L. UV-light-induced aggregation of arsenic and metal sulfide particles in acidic wastewater: The role of free radicals [J]. *Environmental Science & Technology*, 2018, 52(18): 10719–10727.
- [33] PIATAK N M, PARSONS M B, SEAL R R. Characteristics and environmental aspects of slag: A review [J]. *Applied Geochemistry*, 2015, 57: 236–266.
- [34] ANNA P, ERIC D V H, JAKUB K, MALGORZATA G, PIET N L, GILLES G. Copper metallurgical slags—current knowledge and fate: A review [J]. *Critical Reviews in Environmental Science and Technology*, 2015, 45(22): 2424–2486.
- [35] ANNA P, JAKUB K, MALGORZATA G, ARTUR P, ERIC D V H. Weathering of historical copper slags in dynamic experimental system with rhizosphere-like organic acids [J]. *Journal of Environmental Management*, 2018, 222: 325–337.
- [36] GHOSH D, SARKAR S, SENGUPTA A K, GUPTA A. Investigation on the long-term storage and fate of arsenic obtained as a treatment residual: A case study [J]. *Journal of Hazardous Materials*, 2014, 271: 302–310.
- [37] PANTUZZO F L, CIMINELLI V S T. Arsenic association and stability in long-term disposed arsenic residues [J]. *Water Research*, 2010, 44(19): 5630–5640.
- [38] REN J Q, FAN W H, WANG X R, MA Q Q, LI X M, XU Z Z, WEI C Y. Influences of size-fractionated humic acids on arsenite and arsenate complexation and toxicity to *Daphnia magna* [J]. *Water Research*, 2016, 108: 68–77.

## 铜/铅锌冶炼厂硫化砷渣的理化与环境特性

姚理为<sup>1</sup>, 闵小波<sup>1,2</sup>, 徐慧<sup>1</sup>, 柯勇<sup>1,2</sup>, 王云燕<sup>1,2</sup>,  
林璋<sup>1,2</sup>, 梁彦杰<sup>1,2</sup>, 刘德刚<sup>1</sup>, 许秋婧<sup>1</sup>, 何逾洋<sup>1</sup>

1. 中南大学 冶金与环境学院, 长沙 410083;
2. 中南大学 国家重金属污染防治工程技术研究中心, 长沙 410083

**摘要:** 以铜冶炼和铅锌冶炼产生的硫化砷渣为研究对象, 采用 XRD、Raman、SEM-EDS、TG-DTA、XPS 和化学物相分析等检测手段研究其理化特性。采用毒性浸出程序(TCLP)、毒性浸出测试国家标准(CSLT)、三步连续浸提程序(BCR)和批次浸出实验(BLE)分析硫化砷渣的环境稳定性。不同冶炼厂的硫化砷渣理化和环境特性具有明显的差异。物相组成和显微分析表明, ASS-I 主要由超细的絮状颗粒组成, 这种颗粒为粘附有无定型硫的无定型硫化砷。AAS-II 主要组成为无定型硫化砷。两种来源的硫化砷渣中砷均为正三价, 但是硫的价态组成则有所不同。同时, 两种来源的硫化砷渣均具有热不稳定性。TCLP 和 CSLT 结果表明, 浸出液中砷和铅的浸出浓度超过了标准限值。超过 5%和 90%的砷以酸可溶态和可氧化态赋存, 这解释了硫化砷渣浸出毒性高、环境活性强的原因。本研究为铜和铅锌冶炼企业的硫化砷渣的处置提供了全面的信息参考。

**关键词:** 硫化砷渣; 重金属; 理化特性; 环境特性; 浸出毒性

(Edited by Xiang-qun LI)